

Clinical impact of clonal hematopoiesis on severe COVID-19 patients without canonical risk factors

Chang Kyung Kang,^{1*} Baekgyu Choi,^{2*} Sugyeong Kim,³ Choong Hyun Sun,³ Soon Ho Yoon,⁴ Kyukwang Kim,² Euijin Chang,¹ Jongtak Jung,^{1,5} Pyoeng Gyun Choe,¹ Wan Beom Park,¹ Eu Suk Kim,^{1,5} Hong Bin Kim,^{1,5} Nam Joong Kim,¹ Myoung-don Oh,¹ Hogune Im,³ Joohee Kim,⁶ Yong Hoon Lee,⁷ Jaehee Lee,⁷ Hyonho Chun,⁸ Youngil Koh,^{1,3} Ji Yeon Lee,^{6#} Joon Ho Moon,^{7#} Kyoung-Ho Song^{1,5#} and Inkyung Jung^{2#}

¹Department of Internal Medicine, Seoul National University College of Medicine, Seoul; ²Department of Biological Sciences, Korea Advanced Institute of Science and Technology (KAIST), Daejeon; ³Genome Opinion Inc., Seoul; ⁴Department of Radiology, Seoul National University College of Medicine, Seoul; ⁵Department of Internal Medicine, Seoul National University Bundang Hospital, Seongnam; ⁶Division of Pulmonary and Critical Care Medicine, Department of Internal Medicine, National Medical Center, Seoul; ⁷Department of Internal Medicine, Kyungpook National University Hospital, School of Medicine, Kyungpook National University, Daegu and ⁸Department of Mathematical Sciences, Korea Advanced Institute of Science and Technology (KAIST), Daejeon, Republic of Korea

**CKK and BC contributed equally as co-first authors.*

#JYL, JHM, K-HS and IJ contributed equally as co-senior authors.

Correspondence:

J.Y. LEE - fulgeo@nmc.or.kr

J. H. MOON - jhmoon@knu.ac.kr

K.-H. SONG - khsongmd@gmail.com

I. JUNG - ijung@kaist.ac.kr

<https://doi.org/10.3324/haematol.2022.280621>

Supplementary table 1. Clinical characteristics of COVID-19 patients in this study

	CHIP (+) (n = 50)	CHIP (-) (n = 193)
Age, years, median (IQR)	72 (62—81)	65 (52—75)
Male	24 (48.0)	106 (54.9)
Body mass index, mean (\pm SD)	22.5 (\pm 3.4)	24.0 (\pm 3.9)
Underlying diseases		
Diabetes mellitus	12 (24.0)	57 (29.5)
Hypertension	28 (56.0)	97 (50.3)
Chronic kidney disease	5 (10.0)	12 (6.2)
COPD or asthma	2 (4.0)	9 (4.7)
Cerebrovascular disease	8 (16.0)	10 (5.2)
Smoking status		
Unknown	4 (8.0)	18 (9.3)
Never-smoker	34 (68.0)	124 (64.2)
Ex-smoker	8 (16.0)	37 (19.2)
Current smoker	4 (8.0)	14 (7.3)
Worst laboratory findings		
Peak white blood cells, / μ L, median (IQR)	10945 (7780—19153)	9800 (6740—142625)
Lowest lymphocytes, / μ L, median (IQR)	593 (360—932)	771 (492—1340)
Peak monocytes, / μ L, median (IQR)	665 (429—984)	649 (463—869)
Peak C-reactive protein, mg/dL, median (IQR)	11.7 (5.7—18.7)	9.6 (3.2—18.7)
Peak platelet, 10^3 / μ L, median (IQR)	327 (255—421)	320 (236—422)
Lowest hemoglobin, g/dL, median (IQR)	10.4 (8.1—11.8)	11.3 (9.3—13.1)
Peak total protein, g/dL, median (IQR)	6.6 (6.2—7.2)	6.9 (6.5—7.4)
Peak albumin, g/dL, median (IQR)	3.6 (3.4—4.0)	3.8 (3.5—4.2)
Peak blood urea nitrogen, mg/dL, median (IQR)	28.5 (18.8—59.0)	21.0 (14.0—34.8)

Peak creatinine, mg/dL, median (IQR)	0.9 (0.8—1.5)	0.9 (0.7—1.1)
Radiological findings		
Chest X-ray score, baseline, median (IQR)	0.069 (0.018—0.144)	0.046 (0.009—0.113)
Chest X-ray score, peak, median (IQR)	0.178 (0.095—0.246)	0.134 (0.043—0.238)
Pneumonia extent by CT (%), median (IQR)	7.4 (2.3—28.1)	10.3 (2.0—21.2)
Pneumonia weight by CT, g, median (IQR)	192.8 (31.9—461.2)	181.7 (43.1—397.9)
Medical treatment		
Remdesivir	33 (66.0)	79 (40.9)
Steroid	31 (62.0)	92 (47.7)
Hydroxychloroquine	2 (4.0)	15 (7.8)
Lopinavir/ritonavir	10 (20.0)	47 (24.4)
Clinical outcomes		
Severe COVID-19	40 (80.0)	123 (63.7)
Mechanical ventilation	17 (34.0)	29 (15.0)
Death	7 (14.0)	10 (5.2)
Hospital stay, days, median (IQR)	21 (14—33)	15 (10—25)

CHIP, clonal hematopoiesis of indeterminate potential; SD, standard deviation; COPD, chronic obstructive pulmonary disease; IQR, interquartile range; CT, computed tomography

Supplementary table S2. The list of CHIP mutation information of the patients.

Patient	Gene	Chromosome	Position	Variant classification	Reference allele	Alternate allele	Protein change	CDS	VAF	PD
COV008	DNMT3A	chr2	25457242	NON_SYNONYMOUS_CODING	C	T	p.Arg882His	c.2645G>A	2	1
COV010	DNMT3A	chr2	25466797	NON_SYNONYMOUS_CODING	C	T	p.Val636Met	c.1906G>A	2.2	1
COV026	JAK2	chr9	5073770	NON_SYNONYMOUS_CODING	G	T	p.Val617Phe	c.1849G>T	12.1	1
COV028	TET2	chr4	106156562	FRAME_SHIFT	A	AT	p.487Asn_488Aspfs	c.1464_1465insT	2	1
COV028	TET2	chr4	106163991	NON_SYNONYMOUS_CODING	G	T	p.Arg1167Ser	c.3501G>T	5.2	1
COV032	DNMT3A	chr2	25464537	NON_SYNONYMOUS_CODING	C	T	p.Arg659His	c.1976G>A	4.5	0
COV039	GNAS	chr20	57430301	NON_SYNONYMOUS_CODING	G	A	p.Ala661Thr	c.1981G>A	10.6	0
COV048	DNMT3A	chr2	25470502	FRAME_SHIFT	GC	A	p.323Gly_324Thrfs	c.971_972delG	14.9	1
COV057	GNAS	chr20	57484421	NON_SYNONYMOUS_CODING	G	A	p.Arg844His	c.2531G>A	3.6	1
COV063	ASXL2	chr2	25967267	FRAME_SHIFT	TGA	T	p.645Ile_646Thrfs	c.1937_1938delCT	10.2	1
COV064	TET2	chr4	106156427	FRAME_SHIFT	CA	C	p.442Thr_443Thrfs	c.1329_1330delA	3.7	1
COV082	DNMT3A	chr2	25463271	FRAME_SHIFT	G	GC	p.740Ala_741Argfs	c.2221_2222insG	23.7	1
COV082	TET2	chr4	106155920	FRAME_SHIFT	TC	T	p.273Ile_274Asnfs	c.822_823delC	2.7	1
COV090	TET2	chr4	106156121	FRAME_SHIFT	AG	A	p.340Gln_341Glyfs	c.1023_1024delG	3.1	1
COV090	IKZF1	chr7	50468123	NON_SYNONYMOUS_CODING	G	T	p.Ser453Ile	c.1358G>T	2.4	0
COV093	DNMT3A	chr2	25468196	FRAME_SHIFT	A	AT	p.492Ile_493Cysfs	c.1479_1480insA	3	1
COV098	ASXL1	chr20	31022441	FRAME_SHIFT	A	AG	p.642Gly_643Glyfs	c.1927_1928insG	14.2	1
COV100	DNMT3A	chr2	25463574	NON_SYNONYMOUS_CODING	A	T	p.Leu703Gln	c.2108T>A	2.2	0
COV112	DNMT3A	chr2	25463242	NON_SYNONYMOUS_CODING	A	C	p.Phe751Val	c.2251T>G	2.2	1
COV112	ASXL1	chr20	31022441	FRAME_SHIFT	A	AG	p.642Gly_643Glyfs	c.1927_1928insG	19.2	1
COV112	TET2	chr4	106157123	FRAME_SHIFT	C	CA	p.674Ser_675Leufs	c.2025_2026insA	2	1
COV114	TET2	chr4	106155711	FRAME_SHIFT	AG	A	p.204Val_205Leufs	c.613_614delG	5.7	1
COV119	ASXL1	chr20	31022441	FRAME_SHIFT	A	AG	p.642Gly_643Glyfs	c.1927_1928insG	2.1	1
COV120	DNMT3A	chr2	25469147	FRAME_SHIFT	C	CGT	p.436Thr_437Aspfs	c.1310_1311insCA	7.4	1
COV120	SF3B1	chr2	198266834	NON_SYNONYMOUS_CODING	T	C	p.Lys700Glu	c.2098A>G	7.1	1

COV123	PPM1D	chr17	58740374	FRAME_SHIFT	TG	T	p.426Trp_427Profs	c.1280_1281delG	21.5	1
COV124	ASXL1	chr20	31021455	FRAME_SHIFT	CTG	C	p.484Ser_486Alafs	c.1455_1457delTG	2	1
COV127	IDH2	chr15	90633770	NON_SYNONYMOUS_CODING	T	G	p.Gln105Pro	c.314A>C	23.7	0
COV127	ASXL1	chr20	31023054	FRAME_SHIFT	TC	T	p.846Ser_847Thrfs	c.2540_2541delC	23.6	1
COV127	U2AF1	chr21	44514777	NON_SYNONYMOUS_CODING	T	C	p.Gln157Arg	c.470A>G	2.2	1
COV134	DNMT3A	chr2	25469138	STOP_GAINED	C	T	p.Trp440*	c.1320G>A	5.5	1
COV136	DNMT3A	chr2	25457242	NON_SYNONYMOUS_CODING	C	T	p.Arg882His	c.2645G>A	2.6	1
COV141	DNMT3A	chr2	25468121	SPLICE_SITE_DONOR	C	T	-	-	2.1	1
COV143	PPM1D	chr17	58740749	STOP_GAINED	C	T	p.Arg552*	c.1654C>T	2.7	1
COV143	DNMT3A	chr2	25470029	SPLICE_SITE_ACCEPTOR	T	G	-	-	2.9	1
COV147	TET2	chr4	106156935	FRAME_SHIFT	TG	T	p.612Gly_613Glyfs	c.1837_1838delG	3.4	1
COV148	PRPF40B	chr12	50036459	SPLICE_SITE_DONOR	G	A	-	-	5.4	1
COV148	DNMT3A	chr2	25467449	NON_SYNONYMOUS_CODING	C	A	p.Gly543Cys	c.1627G>T	3.2	1
COV151	BCOR	chrX	39932965	NON_SYNONYMOUS_CODING	G	T	p.Pro545Gln	c.1634C>A	26.3	0
COV158	DNMT3A	chr2	25467209	SPLICE_SITE_ACCEPTOR	T	C	-	-	2.8	1
COV158	U2AF1	chr21	44524456	NON_SYNONYMOUS_CODING	G	A	p.Ser34Phe	c.101C>T	2.7	1
COV163	STAG2	chrX	123159763	NON_SYNONYMOUS_CODING	G	T	p.Gly40Cys	c.118G>T	20.2	0
COV164	DNMT3A	chr2	25470498	NON_SYNONYMOUS_CODING	G	A	p.Arg326Cys	c.976C>T	2.4	1
COV167	TET2	chr4	106196213	STOP_GAINED	C	T	p.Arg1516*	c.4546C>T	17.6	1
COV174	DNMT3A	chr2	25470458	SPLICE_SITE_DONOR	AC	A	-	-	7	1
COV187	NF1	chr17	29556889	STOP_GAINED	C	T	p.Gln963*	c.2887C>T	7.6	1
COV190	JAK2	chr9	5073770	NON_SYNONYMOUS_CODING	G	T	p.Val617Phe	c.1849G>T	20.9	1
COV196	IDH2	chr15	90633770	NON_SYNONYMOUS_CODING	T	G	p.Gln105Pro	c.314A>C	24	0
COV196	ASXL1	chr20	31023054	FRAME_SHIFT	TC	T	p.846Ser_847Thrfs	c.2540_2541delC	26.6	1
COV196	U2AF1	chr21	44514777	NON_SYNONYMOUS_CODING	T	C	p.Gln157Arg	c.470A>G	2.3	1
COV200	DNMT3A	chr2	25469138	STOP_GAINED	C	T	p.Trp440*	c.1320G>A	5.8	1
COV201	DNMT3A	chr2	25457242	NON_SYNONYMOUS_CODING	C	T	p.Arg882His	c.2645G>A	3	1
COV203	DNMT3A	chr2	25457270	FRAME_SHIFT	G	GGA	p.871Val_872Hisfs	c.2616_2617insCT	4.2	1
COV206	PPM1D	chr17	58740374	FRAME_SHIFT	TG	T	p.426Trp_427Profs	c.1280_1281delG	15.5	1

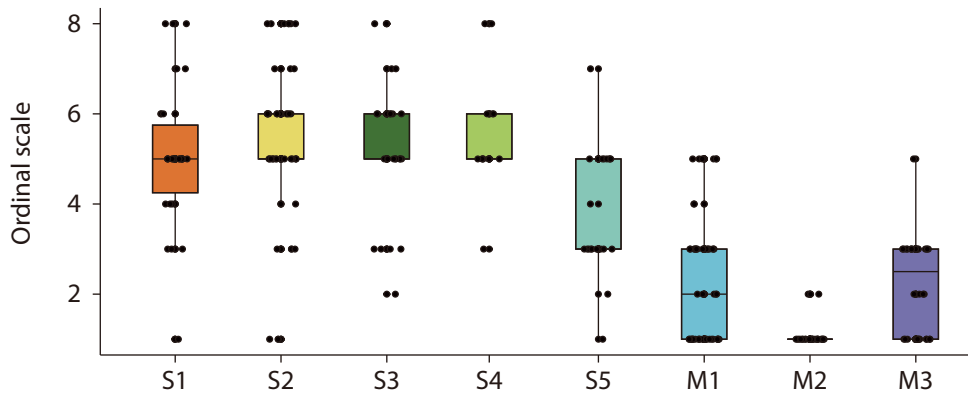
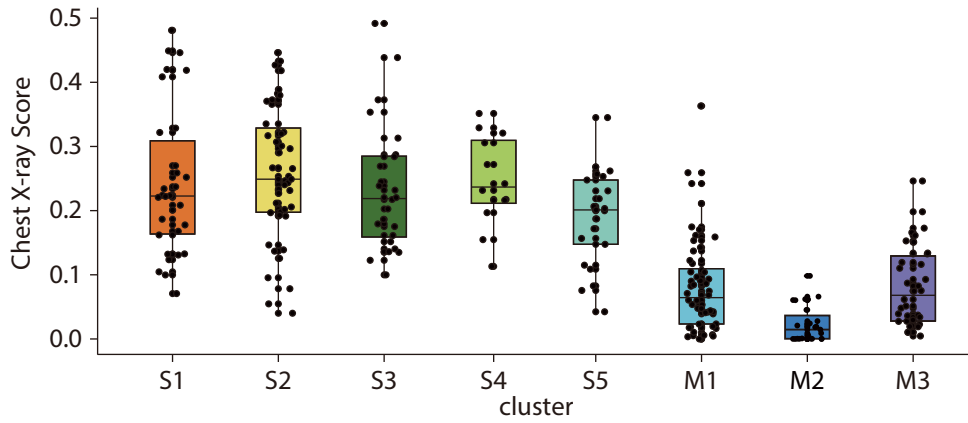
COV215	U2AF1	chr21	44513271	NON_SYNONYMOUS_CODING	C	T	p.Gly222Ser	c.664G>A	2.3	0
COV217	CBL	chr11	119149280	NON_SYNONYMOUS_CODING	G	A	p.Val430Met	c.1288G>A	2.3	0
COV217	TET2	chr4	106190830	NON_SYNONYMOUS_CODING	G	A	p.Gly1370Arg	c.4108G>A	2.6	1
COV221	DNMT3A	chr2	25469037	NON_SYNONYMOUS_CODING	C	T	p.Arg474His	c.1421G>A	5.6	0
COV223	PPM1D	chr17	58740749	STOP_GAINED	C	T	p.Arg552*	c.1654C>T	2.9	1
COV223	TET2	chr4	106164086	SPLICE_SITE_DONOR	T	C	-	-	28.8	1
COV224	DNMT3A	chr2	25463307	NON_SYNONYMOUS_CODING	C	T	p.Arg729Gln	c.2186G>A	16.1	1
COV225	DNMT3A	chr2	25463237	NON_SYNONYMOUS_CODING	G	T	p.Phe752Leu	c.2256C>A	2.6	0
COV235	TET2	chr4	106190818	NON_SYNONYMOUS_CODING	C	G	p.Arg1366Gly	c.4096C>G	2.3	0
COV238	DNMT3A	chr2	25458663	STOP_GAINED	G	T	p.Ser837*	c.2510C>A	3.3	1
COV239	ASXL1	chr20	31021211	STOP_GAINED	C	T	p.Arg404*	c.1210C>T	4.4	1
COV243	DNMT3A	chr2	25468187	NON_SYNONYMOUS_CODING	A	G	p.Cys497Arg	c.1489T>C	6.2	0
COV254	DNMT3A	chr2	25459806	NON_SYNONYMOUS_CODING	T	C	p.Lys826Arg	c.2477A>G	3.6	1
COV254	DNMT3A	chr2	25470497	NON_SYNONYMOUS_CODING	C	T	p.Arg326His	c.977G>A	17.5	0
COV262	TET2	chr4	106156729	STOP_GAINED	C	T	p.Arg544*	c.1630C>T	5.1	1
COV264	ASXL1	chr20	31021118	STOP_GAINED	C	T	p.Gln373*	c.1117C>T	16.7	1
COV264	BRCC3	chrX	154348327	STOP_GAINED	C	T	p.Gln285*	c.853C>T	18.1	1
COV270	SRSF2	chr17	74732959	NON_SYNONYMOUS_CODING	G	T	p.Pro95His	c.284C>A	8.1	1

Supplementary Fig. 1. Distribution of representative clinical factors in COVID-19 patients and contribution of each chronic risk factor in COVID-19 severity

A Boxplots showing distribution of Chest X-ray score and Ordinal scale in eight clusters defined in Figure 1B. For the boxplots, the box represents the interquartile range (IQR) and the whiskers correspond to the highest and lowest points within $1.5 \times \text{IQR}$. Statistical significance was not examined. Color indicates the cluster, and dot indicates one patient. **B** Barplot showing logistic regression weight (coefficient) of each chronic risk factor in predicting COVID-19 severity. The regression weight of CHIP is highlighted with yellow. Green indicates positive value, while Red indicates negative value. COPD, Chronic obstructive pulmonary disease.

Supplementary Figure 1.

A



B

